

3D porous media liquid-solid interaction simulation using SPH modeling and Tomographic images

Alfonso Gastelum Strozzi
University of Auckland
Auckland, New Zealand
agas012@aucklanduni.ac.nz

Jorge Marquez
CCADET, UNAM
Mexico, Mexico
jorge.marquez@ccadet.unam.mx

Flavio Trujillo
HRAEO
Oaxaca, Mexico
flaviotrujillo@gmail.com

Celine Duwig
IRD/LTHE
Grenoble, France
cduwig@yahoo.fr

Blanca Prado
Department of Geology, UNAM
Mxico City, Mxico
blancaprado@yahoo.com.mx

Pavan Gamage
University of Auckland
Auckland, New Zealand
pavan.gamage@gmail.com

Patrice Delmas
University of Auckland
Auckland, New Zealand
patrice@cs.auckland.ac.nz

Abstract

We propose to study the mechanical properties of a volcanic soil sample (monolith) using a computer model. We propose the use of CT-images to construct the Mechanical Computational Model. The image obtained from the CT-Scan give us a 3D model of the pores system of the monolith. This system relates the internal connectivity between different pores and the soil volume. To simulate fluid-solid interaction and the mechanical properties of the soil monolith model we used Smoothed Particle Hydrodynamics. This method has a proven track report to solve multistate interaction. As SPH relies on a set of points without using a Tetrahedral Mesh representation, we can relate easily the intensity value of each pixel of the CT-Scan images (related to density values) to our 3D point data set. We aim to our 3D pore network model and the SPH evolution modelling technique to simulate the fate of solutes in porous media. Such study is of importance to the soil sciences community to accurately predict the impact of pollutants and chemical compounds in groundwater supplies.

1 Introduction

Solute transport (contained in rain or/and irrigation water) through soil is widely researched and of public concern as aquifers are progressively contaminated by chemicals (both agricultural and pharmaceutical-mostly antibiotics) around the world. The reliable prediction of the transport of contaminants through soils is a challenging mandatory step to manage land and protect underground water resources [3]. Classical transport equations are for homogeneous soil structure and uniform flow that is controlled by convection and dispersion. In reality, solute transport is dependent on the non-uniformity of soils with a mostly heterogeneous distribution of solute transport [4]. The main impediment for developing good predictive models is the limited understanding of the mechanisms that govern transport. We must be able to take into account the

complexity of soil structure and porous networks. Still, the increasing availability of non destructive imaging techniques (X-ray tomography, PET), advanced Image Processing and physical modelling make the development of advanced 3D simulation model possible. In this work we introduce an SPH-based 3D soil core monolith simulation model combined with Image processing techniques to study different conditions of fluid-solid interactions. The surface information of the topology and the internal pores that form the monolith will be obtained using images obtained from a CT-Scan. The information of the Ct-Scan will also be used to obtain the relation density-pixel intensity level. To build the model of the soil monolith we using CT-Scan images as our initial 2D surfaces we look at the graph of a 3D connectivity for each pixel representing a pore wall monolith. The behaviour of the soil pore network and the interaction with fluids is solved using a modified SPH (Smooth Particle Hydrodynamics)[1] algorithm that gives the solution to the governing dynamic equations.

The main contribution of this paper is the integration of our 3D model obtained from CT-Scan images and a Mechanical model based on SPH equations.

2 CT-Scan Information

The data to construct the model is obtained from a CT-Scan system. The images will give us the internal composition of the monolith. The resolution of the CT-Scan generates a 512 cubic voxels volume with a 50 microns per voxel resolution. This resolution allows us to see the different pores structures in the soil and to cover the full range of macro-pores (size) help responsible for the infiltration of solutes in aquifers. The intensity level of each pixel will be used to obtain the density value of the different components in the soil.

The pores are obtained using an edge detection algorithm based on Deriche edge extractor algorithm [2] with results show in Figure 1.

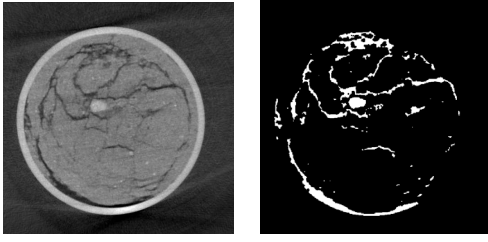


Figure 1: Left: Original CT-Scan image, Right: Iso-surface obtained from the contour detection and segmentation.

3 2D/3D Model

We first need to delineate the iso-contours required to build our initial 2D/3D point data. We use an edge detection algorithm to obtain the coordinates of the pixels that represent the walls of the pores. The first imaging experiments are obtained using a transversal cut of the CT-scan to obtain a 2D model of the soil wall Figure 2.

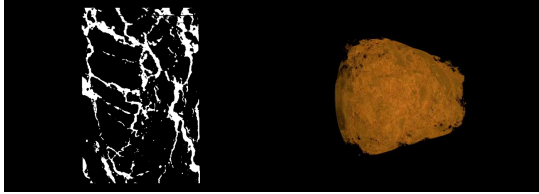


Figure 2: Left: Transversal wall of the monolith; Right: 3D representation of the pores structures inside the monolith.

Figure 3 displays a transversal cut of the soil monolith used to build a Particles System which will represent the pore network solid walls.

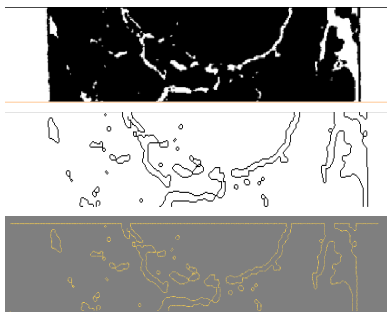


Figure 3: Left: Transversal wall of a section of the soil monolith; Center: Contour segmentation of the pores walls; Right: Particle system of the pores walls in the soil.

Figure 4 shows the 3D point representation obtained from a set of 2D CT-Scan images. The edges detected from the iso-contours of the soil volume are used as input data. The walls forming the pores are connected using a 26-connectivity algorithm. The walls also identify isolated pores.

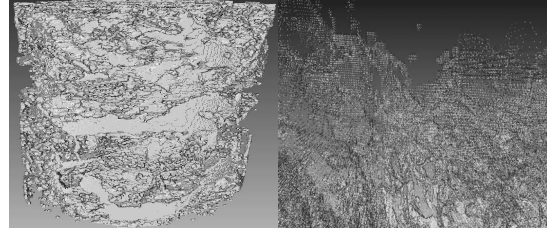


Figure 4: Left: 3D point system of the soil monolith, Right: A magnified close shot of the point system.

4 Particle System

Our mechanical model is based on a particle system. In this section we present the technique from which our particle system derives. We will also have a look at the different properties of the soil and the fluids interacting with it. The particle system represents discrete volume as fractions of the total volume of the object. Each one of these particles has mechanical properties that describe its behaviour.

The system is based on the point system (obtained from the contour of the CT-scan images) and on a description of their connectivity that gives us which pixels are parts of the same wall. We define different conditions to obtain separate groups of particles. Separate groups of particles define the soil solid components while another group defines the internal constituents of the pores. The latter group has the finality to be able to define the quantities of air and fluid within the soil core studied.

5 Mechanical Model: Smoothed Particle Hydrodynamics

Smoothed Particle Hydrodynamics is a Lagrangian approach used to solve fluid-related and astronomical problems. Here, we add governing laws of soil mechanics to cater for the soil-pore structure and expected behaviour. The solid and fluid components of the soil core are defined by a set of n particles i and j , with individual mass m_i and density ρ_i . The continuous integral representation is replaced by a discrete summation over all the neighboured particles j :

$$A(r) = \sum_j m_j \frac{A_j}{\rho_j} W(r - r_j, h), \quad (1)$$

where $A(r)$ is the function value at location r and $W(r - r_j, h)$ is a smoothing kernel and h its radius of interaction[1]. The gradient of function A_i for the particle i can be computed as:

$$\nabla A_i = \frac{1}{\rho_i} \sum_j m_j (A_j - A_i) \nabla W(r_i - r_j, h), \quad (2)$$

We use the smoothing kernel defined in [?]:

$$W(r, h) = \begin{cases} c \frac{2h}{\pi} \cos\left(\frac{(r+h)\pi}{2h}\right) + c \frac{2h}{\pi}, & 0 \leq r \leq h \\ 0, & \text{otherwise} . \end{cases}$$

$$c = \frac{\pi}{8h^4 \cdot \left(\frac{\pi}{3} - \frac{8}{\pi} + \frac{16}{\pi^2}\right)} \quad (3)$$

In their initial state, all particles are considered to be immobile. The continuity of the system is ensured by constructing a neighbourhood for each particle. The amount of neighbours is determined using the smooth particles technique. Two particles are neighbours if $D_{ij} < scale \cdot \zeta_{ij}$ with D_{ij} the distance between particles and ζ_{ij} given by:

$$\zeta_{ij} = \frac{h_i + h_j}{2}. \quad (4)$$

Here, h_i , h_j are the smoothing lengths of the particles and the scale factor is used to adjust the number of neighbour particles within a given neighbourhood. The neighbourhood search is performed using an Octree algorithm. The same Octree algorithm will later compute particles collision. The initial mass property for each particle is set using a density value of ρ . From there the density value is adapted using the pixel intensity values of the CT-scan images.

The density changes over time depending on the particle configuration and is defined as:

$$\rho_i = \sum_j m_j W(r_i - r_j, h). \quad (5)$$

The particle system behaves following the rules of continuum mechanics. We need to define the rule equation for the different systems depending on their solid-liquid state.

5.1 Internal Forces: Fluids

For fluids we use a simplified Navier-Stokes equation for incompressible fluids to describe how the particles behaved. This equation can be expressed as shown in 7 where a corresponds to the acceleration and is integrated using the Leap-Frog scheme [7].

$$\rho \left(\frac{\partial v}{\partial t} + v \cdot \nabla v \right) = -\nabla p + \rho g + \mu \nabla^2 v. \quad (6)$$

$$\rho a = f^{pressure} + f^{external} + f^{viscosity}. \quad (7)$$

The internal forces due to pressure and viscosity are obtained using the following equations:

$$f_i^{pressure} = - \sum_j m_j \frac{p_i + p_j}{2\rho_j} \nabla W(r_{ij}, h) \quad (8)$$

$$f_i^{viscosity} = - \sum_j m_j \frac{\mu_i + \mu_j}{2} \frac{v_i + v_j}{\rho_j} \nabla^2 W(r_{ij}, h) \quad (9)$$

5.2 Internal Forces: Solids

The internal forces of the body are defined by their respective constitutive equation and the interaction of their particles [8], this forces is the one that oppose to the movement of an individual particle due to the interaction with the neighbourhood ones. This force is obtained using the strain energy U_i (potential energy stored in each particle) for the particles and is defined as:

$$U_i = \frac{1}{2} V_i (\epsilon_i \cdot \sigma_i), \quad (10)$$

where V_i is the volume of the particle obtained using the density value 5, ϵ_i is the strain and σ_i the stress.

The relation between strain and stress for an elastic material is given by the Hooke's law:

$$\sigma = K \epsilon, \quad (11)$$

where K is the elastic modulus and ϵ is given by

$$\nabla \epsilon = \nabla \chi + \nabla \chi^T + \nabla \chi \chi^T. \quad (12)$$

Here, $\nabla \chi$ is the gradient of the vector displacement with respect to the original position of the particles. The force that is been exert over the particle j by i is defined as:

$$\begin{aligned} F_{ji} &= -\nabla \chi_i U_i = -V_i \sigma_i \nabla \chi_j \epsilon_i \\ F_{ji} &= -2V_i (I + \nabla \chi_i^T) \epsilon_i \frac{\partial \nabla \chi_i}{\partial \chi_j}. \end{aligned} \quad (13)$$

We can express this equation using the SPH function and its gradient 2 to obtain

$$\nabla \chi_i = \frac{1}{\rho_i} \sum_j m_j (\chi_j - \chi_i) \nabla W(r_{ij}, h). \quad (14)$$

So far we consider external forces dealing with collisions from particles belonging to different objects. The principal external forces to consider are obtained from the fluid-soil (solid) interaction. Another external force to consider is the pore water pressure that can modify the soil wall structure.

6 Octree Algorithm

In order to obtain a fast computational solution we implemented a modified octree-space search algorithm (described in Figure 5). We used the initial space neighbours to classify groups of particles, then built a branch of the tree containing the particles that are neighbours in space (this vicinity is different from the one used for SPH). This helps organise the neighbour data and accelerates the SPH computation process. Each branch of the octree contains the particles situated in a specific volume region (in our case a cube). The number of particles and the total volume they represent depends on the scale-level of the branch. Each branch is a new discrete volume representation (considered as a particle at the current scale), with an associated mass equal to the sum of all the particles' mass contained in the considered branch. The object's volume is represented here as a discrete approximation (as in Figure 5), The higher the scale-level, the less accurate the approximation. The associated discrete volume has a new smooth kernel and vicinity which is computed considering only branches at the same scale-level.

7 Results

The Figures 6 and 7 shows the result of water particles interacting with the monolith model. The water model models the paths taken through the soil pores network. The behaviour of the Particles System is controlled by the equations presented in this paper.

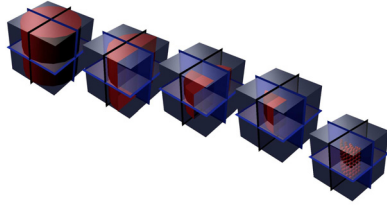


Figure 5: Octree sub-division. From left to right: multi-scale representation of a multi-particle object.

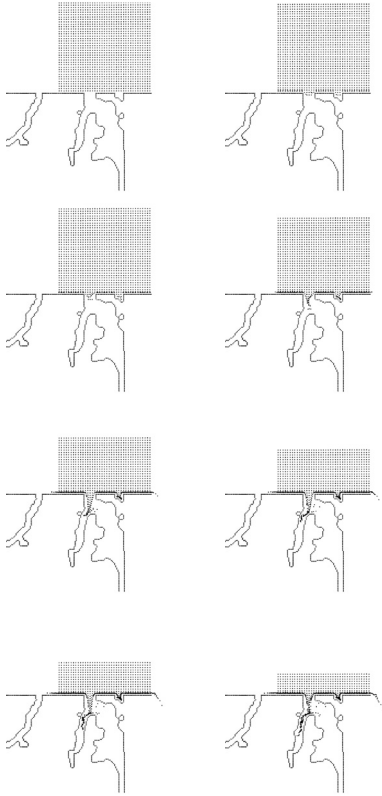


Figure 6: The images show the result of the 2D interaction of the water particles and the solid.

8 Conclusions

We presented here a method to simulate 3D interactions between fluid and solid particles within the pore network of a porous media core. First, 3D data is acquired by non invasive 3D acquisition systems such as CT-Scans. Next the data is segmented to extract a network of points which define the pore walls within any given soil core. SPH equations provide a framework to realise dynamic soli-liquid interaction with the soil core pore network. The advantage of the particle system is the possibility of creating a more complex system than previously introduced with surface models. Instead of the equations currently used we could define more complex solutions to solve different problems using the same SPH approach. The SPH model and its constitutive modelling technique determine the resulting internal response to the forces in presence and the changes in the fluid behaviour travelling inside the pores. An interesting challenge would be to compare the results obtained from the particles model with the

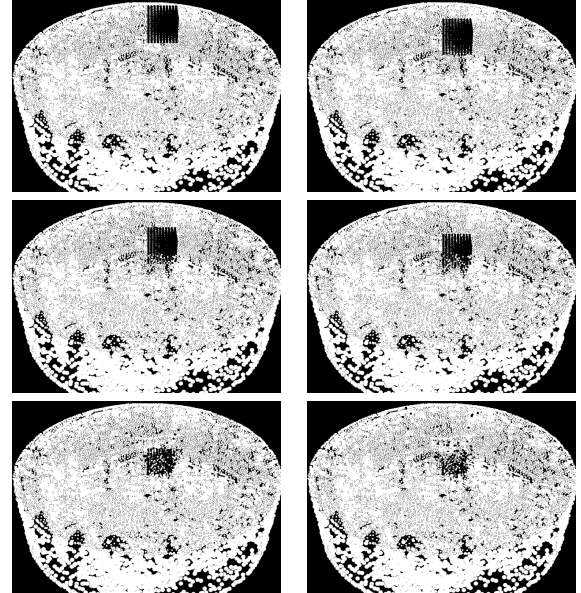


Figure 7: The images show the result of the 3D interaction of the water particles and the solid.

ones obtained from other mathematical solutions as for example with Finite Element Methods. We aim to assess our simulation technique comparing results of water flow experiments through a given porous media sample to its 3D model performance.

References

- [1] J. J. Monaghan, "Smoothed particle hydrodynamics", *Annual Review of Astronomy and Astrophysics*, vol.30, pp.543-574, 1992.
- [2] R. Deriche, "Using Canny's criteria to derive a recursively implemented optimal edge detector", *International Journal of Computer Vision*, vol.1, no.2, pp.167-187, 1987.
- [3] N. J. Jarvis, "A review of non-equilibrium water flow and solute transport in soil macropores: principles, controlling factors and consequences for water quality", *European Journal of Soil Science*, vol.58, pp.523-546, 2007.
- [4] H. Fluhler, W. Durner, and M. Flury, "Lateral solute mixing processes – A key for understanding field-scale transport of water and solutes", *Geoderma*, vol.70, pp.165-183, 1996.
- [5] W. E. Lorensen, and H. E. Cline, "Marching Cubes: a high resolution 3D surface reconstruction algorithm", *Computer Graphics*, vol.21, no.4, pp.163-169, 1987.
- [6] D. K. Cassel, J. M. Brown and G. A. Johnson, "Computer tomographic analysis of water distribution and flow in porous media", *Journal Theoretical and Applied Climatology*, vol.42, no.4, pp.223-228, 2004.
- [7] G. R. Liu, M. B. Liu, and S. Li, "Smoothed particle hydrodynamics a meshfree method", *Computational Mechanics*, vol.33, pp.491-491, 2004.
- [8] B. Solenthaler, J. Schffli, and R. Pajarola, "A Unified Particle Model for Fluid-Solid Interactions", *Computer Animation and Virtual Worlds*, vol.18, no.1, pp. 69-82, 2007.
- [9] M. Mller, S. Schirm, M. Teschner, B. Heidelberger, and M. Gross, "Interaction of fluids with deformable solids", *Journal of Computer Animation and Virtual Worlds*, vol.15, no.3-4, pp. 159-171, 2004.